

Modeling of Si self-diffusion in SiO₂: Effect of the Si/SiO₂ interface including time-dependent diffusivity

Masashi Uematsu,^{a)} Hiroyuki Kageshima, and Yasuo Takahashi
NTT Basic Research Laboratories, NTT Corporation, Atsugi 243-0198, Japan

Shigeto Fukatsu and Kohei M. Itoh
*Department of Applied Physics and Physico-Informatics and CREST-JST, Keio University,
 Yokohama 223-8522, Japan*

Kenji Shiraishi
Institute of Physics, University of Tsukuba, Tsukuba 305-8571, Japan

Ulrich Gösele^{b)}
Div. Engineering & Applied Sciences, Harvard University, Cambridge, Massachusetts 02138

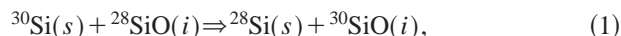
(Received 9 October 2003; accepted 3 December 2003)

Self-diffusion of Si in thermally grown SiO₂ is modeled taking into account the effect of SiO molecules generated at the Si/SiO₂ interface and diffusing into SiO₂ to enhance the self-diffusion. Based on the model, a recent self-diffusion experiment of ion-implanted ³⁰Si in SiO₂, which showed increasing self-diffusivity with decreasing distance between the ³⁰Si diffusers and Si/SiO₂ interface [Fukatsu *et al.*, *Appl. Phys. Lett.* **83**, 3897 (2003)], was simulated, and the simulated results fit the experimental profiles. Furthermore, the simulation predicts that the self-diffusivity would increase for a longer annealing time because more SiO molecules should be arriving from the interface. Such time-dependent diffusivity was indeed found in our follow-up experiments, and the profiles were also fitted by the simulation using a single set of parameters. © 2004 American Institute of Physics. [DOI: 10.1063/1.1644623]

With the scaling down of Si devices, the bulk materials of interest are closer to material interfaces. Therefore, even phenomena in bulk materials, such as diffusion, are more likely to be affected by interfaces, such as the Si/SiO₂ interface. Recently, we have obtained the experimental result that the distance from the Si/SiO₂ interface has a strong influence on Si self-diffusion in SiO₂.¹ In this letter, we constructed a model in which SiO molecules generated at the interface and diffusing into SiO₂ enhance Si self-diffusion in SiO₂. Based on the model, we simulated the diffusion profiles of ion-implanted ³⁰Si in SiO₂ for various temperatures and SiO₂ thicknesses in a unified manner. In addition, the simulation predicts the possibility of time-dependent diffusivity, which indeed was experimentally observed in this study.

In our previous experiment,¹ we showed that the self-diffusivity obtained from the diffusion profile of implanted ³⁰Si in ²⁸SiO₂, assuming a constant diffusion coefficient, increases with decreasing ²⁸SiO₂ thickness, i.e., the distance between the diffusing ³⁰Si species and ²⁸Si/²⁸SiO₂ interface, when silicon-nitride capping layers are placed on top of the SiO₂. In contrast, the self-diffusivity of uncapped samples annealed in flowing argon with 1% oxygen showed no significant dependence on the ²⁸SiO₂ thickness, and the diffusivity values agreed with the thermal equilibrium values reported by us, which were determined using ^{nat}SiO₂/²⁸SiO₂ structures.² (^{nat}Si refers to Si with the natural isotopic abundance.) As the possible origins of the distance dependence of Si self-diffusion, we have examined the effect of nonstoichi-

ometry (excess Si in SiO₂) claimed in Refs. 3 and 4 and the effect of lattice damage due to implantation. We have also evaluated the stress due to silicon-nitride capping layer. However, none of these effects is large enough to induce the large enhancement of the silicon self-diffusivity (a factor-of-6 enhancement between 200 and 650 nm from the interface). These experimental results lead us to conclude that Si species generated at the Si/SiO₂ interface and diffusing into SiO₂ enhance the Si self-diffusion. There have been a number of suggestions, based on experimental speculations and theoretical predictions, regarding emission of Si species from the Si/SiO₂ interface to SiO₂.⁵⁻¹¹ In our view, SiO generated at the Si/SiO₂ interface via the reaction Si + SiO₂ → 2SiO^{5,6} is the most likely candidate as the dominant Si species. In the uncapped sample, oxygen diffusing from the surface reacts with the SiO near the interface and the SiO cannot reach the region where ³⁰Si diffusion is taking place. Therefore, there is no enhancement of Si self-diffusion and only thermal equilibrium self-diffusion is observed. On the other hand, for the capped sample, where the cappings act as perfect barriers against oxygen incorporation, the SiO generated diffuses into the region of implanted ³⁰Si. Therefore, the enhanced self-diffusion via the SiO is observed together with the thermal self-diffusion. Consequently, we propose a mechanism of Si self-diffusion in SiO₂ enhanced by the existence of SiO via the reaction such that

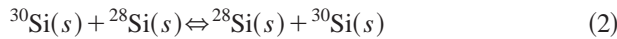


where Si atoms substituted in the Si sites of SiO₂ [denoted as (s)] diffuse via the kick-out reaction with diffusing SiO mol-

^{a)}Electronic mail: uematsu@aecl.ntt.co.jp

^{b)}On sabbatical leave from: Max Planck Institute, Halle, Germany.

ecules in interstitial sites [denoted as (i)]. In addition to Eq. (1), a simple Si self-diffusion mechanism via Si interstitials or vacancies



is taken into account for the thermal equilibrium self-diffusion mentioned above.

The model described above leads to the following set of coupled partial differential equations to describe self-diffusion of ^{30}Si in $^{28}\text{SiO}_2$:

$$\partial C_{^{30}\text{Si}} / \partial t = \partial / \partial x (D_{\text{Si}}^{\text{SD}} \partial C_{^{30}\text{Si}} / \partial x) - R \quad (3)$$

$$\partial C_{^{30}\text{SiO}} / \partial t = \partial / \partial x (D_{\text{SiO}} \partial C_{^{30}\text{SiO}} / \partial x) + R \quad (4)$$

$$\partial C_{^{28}\text{SiO}} / \partial t = \partial / \partial x (D_{\text{SiO}} \partial C_{^{28}\text{SiO}} / \partial x) - R, \quad (5)$$

where R is the reaction term for Eq. (1) given by

$$R = k_f C_{^{30}\text{Si}} C_{^{28}\text{SiO}} - k_b C_{^{30}\text{SiO}}. \quad (6)$$

The Si self-diffusivity is, as a whole, described by

$$D_{\text{Si}}^{\text{SD}} = D_{\text{Si}}^{\text{SD}}(\text{th}) + D_{\text{SiO}}^{\text{SD}} C_{^{28}\text{SiO}} / C_{\text{SiO}}^0. \quad (7)$$

In these equations, C_x is the concentration of the corresponding species in Eqs. (1) and (2), $D_{\text{Si}}^{\text{SD}}(\text{th})$ the thermal Si self-diffusivity, D_{SiO} the diffusivity of SiO, and k_f and k_b are the forward and backward rate constants of Eq. (1). In Eq. (7), $D_{\text{SiO}}^{\text{SD}} = D_{\text{SiO}} C_{\text{SiO}}^0 / N_0$ is the self-diffusivity of silicon via SiO molecules, where N_0 denotes the number of SiO₂ molecules in a unit volume of silicon oxide. Here, C_{SiO}^0 denotes the maximum concentration of SiO interstitials in SiO₂ and is described as $C_{\text{SiO}}^0 = 3.6 \times 10^{24} \exp(-1.07 \text{ eV}/kT)$, which is estimated from the product of the interstitial segregation coefficient for the Si/SiO₂ interface¹² and the equilibrium self-interstitial concentration in Si.¹³ In Eq. (3), the thermal self-diffusion [Eq. (2)] is represented by the diffusion term with $D_{\text{Si}}^{\text{SD}}(\text{th})$, which is independent of $C_{^{30}\text{Si}}$,^{2,4} and the experimentally obtained $D_{\text{Si}}^{\text{SD}}(\text{th}) = 0.8 \exp(-5.2 \text{ eV}/kT)$ ² is used for the simulation. The boundary condition for $^{28}\text{SiO}(i)$ at the $^{28}\text{Si}/^{28}\text{SiO}_2$ interface is given by $C_{^{28}\text{SiO}(i)}(x=\text{interface}) = C_{\text{SiO}}^0$ to describe the generation of SiO at the interface. The amount of $^{30}\text{SiO}(i)$ arriving at the $^{28}\text{Si}/^{28}\text{SiO}_2$ interface is so small that the mixing of ^{28}Si with ^{30}Si at the interface is neglected. The boundary condition at the nitride-capped surface is represented by a zero-flux condition because the capings act as barriers. Reaction (1) is assumed to be so fast that the local equilibrium of the reaction is established, and hence the rate constants are set to be large enough. In addition, Si and SiO₂ are thermodynamically in equilibrium with SiO with a certain solubility in SiO₂, which only depends on temperature. At the interface, therefore, SiO is generated until this solubility value has been reached and a higher concentration of SiO leads to decomposition of SiO into Si and SiO₂. Interfacial reactions are generally much faster than one-dimensional diffusion away from an interface. Therefore, we assume that the generation rate of SiO at the interface is large enough so that the SiO concentration at the interface is fixed at C_{SiO}^0 . The only parameter deduced from the simulation to fit the experimental profiles of ^{30}Si is D_{SiO} . Equations (3)–(6) were solved numerically by the partial differential equation solver ZOMBIE.¹⁴

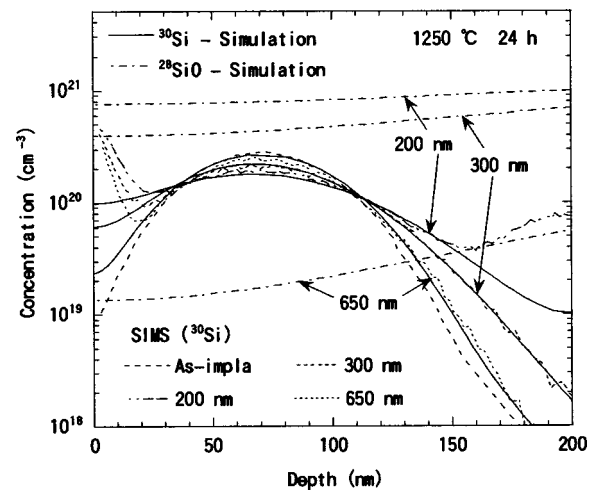


FIG. 1. Simulated and experimental ^{30}Si depth profiles and simulated ^{28}SiO profiles after annealing of 24 h at 1250 °C. The as-implanted profile is also shown as a reference. In SIMS data, the increase of ^{30}Si concentration close to the surface (0–20 nm) is an artifact from silicon-nitride caps, and that deep in the bulk (>160 nm) in the 200-nm-thick sample is ^{30}Si that diffused from ^{nat}Si substrates (800 nm below the ^{28}Si epilayer) during the thermal oxidation to prepare the sample.

We simulated the diffusion profiles of ion-implanted ^{30}Si in $^{28}\text{SiO}_2$ in nitride-capped samples measured as a function of the temperature (1150, 1200, and 1250 °C) and $^{28}\text{SiO}_2$ thickness (200, 300, and 650 nm). The experimental procedure is described in our previous letter.¹ Thermally grown $^{28}\text{SiO}_2$ samples were implanted with ^{30}Si at 50 keV to a dose of $2 \times 10^{15} \text{ cm}^{-2}$ and capped with a 30-nm-thick silicon nitride layer. Figure 1 shows the simulated and experimental ^{30}Si depth profiles after annealing for 24 h at 1250 °C. For the simulated ^{30}Si profiles, the concentration of $^{30}\text{Si}(s)$ is shown because it is about two orders of magnitude larger than that of $^{30}\text{SiO}(i)$. The simulation results fit the experimental profiles of ^{30}Si for all $^{28}\text{SiO}_2$ thicknesses using the same parameter values. This is in contrast to the self-diffusivity obtained by a simple fitting, or under the assumption of a constant diffusion coefficient for each profile, which increases with decreasing $^{28}\text{SiO}_2$ thickness: 6×10^{-17} , 4×10^{-17} , $1 \times 10^{-17} \text{ cm}^2/\text{s}$ for 200, 300, 650 nm, respectively (the contribution from $D_{\text{Si}}^{\text{SD}}(\text{th})$ at 1250 °C is $5 \times 10^{-18} \text{ cm}^2/\text{s}$ for all thicknesses). For other temperatures, the simulation results also fit the ^{30}Si profiles for all $^{28}\text{SiO}_2$ thicknesses using the same parameter values for each temperature. In Fig. 1, the profiles of ^{28}SiO obtained from the simulation are also shown. As expected from Eq. (1), ^{28}SiO with higher concentration leads to larger enhancement of ^{30}Si diffusion. The ^{28}SiO concentration in the ^{30}Si region increases with decreasing the $^{28}\text{SiO}_2$ thickness. This is the reason the ^{30}Si self-diffusivity, assuming a constant diffusion coefficient, increases with decreasing $^{28}\text{SiO}_2$ thickness. This thickness dependence arises because the SiO diffusion is so slow that the ^{28}SiO concentration at the ^{30}Si region critically depends on the distance from the interface, where the SiO is generated.

The value of D_{SiO} was deduced from the fittings and is described as $D_{\text{SiO}} = 3.4 \times 10^2 \exp(-5.2 \text{ eV}/kT)$. The temperature dependence of the D_{SiO} is shown in Fig. 2, together with that of the thermal equilibrium self-diffusivity, $D_{\text{Si}}^{\text{SD}}(\text{th})$,^{2,15,16} and that of the SiO diffusivities reported in

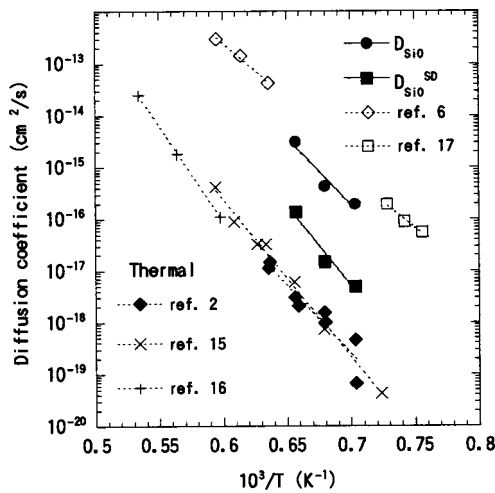


FIG. 2. Temperature dependencies of the Si diffusion coefficients obtained in this study with those reported previously in the literature. Filled circles (●) and filled squares (■) represent the present results for D_{SiO} and $D_{\text{SiO}}^{\text{SD}}$, respectively. The previously reported values are $D_{\text{Si}}^{\text{SD}}(t_{\text{th}})$ from Refs. 2 (in thermally grown SiO_2), 15 (fused silica), and 16 (quartz), and the SiO diffusivities from Refs. 6 and 17 (thermally migrated impurities and defect evolutions as markers, respectively).

Refs. 6 and 17. In Fig. 2, $D_{\text{SiO}}^{\text{SD}} = 4 \times 10^4 \exp(-6.2 \text{ eV}/kT)$ obtained in this study, which has an activation energy comparable to that of $D_{\text{Si}}^{\text{SD}}(t_{\text{th}})$, is also plotted. The D_{SiO} is comparable to the SiO diffusivities reported in Refs. 6 and 17 (thermally migrated impurities and defect evolutions as markers, respectively) within a factor of 5, which can be regarded as a reasonable agreement. Our findings imply that the Si/SiO_2 interface could influence silicon processes involving Si self-diffusion. The D_{SiO} value deduced has the value of $\sim 4 \times 10^{-17} \text{ cm}^2/\text{s}$ at 1100°C , and the diffusion length for 10 s annealing is $2(D_{\text{SiO}} \times t)^{1/2} \sim 0.4 \text{ nm}$. This estimation indicates that SiO from the interface may affect the phenomena in the bulk in nitride-capped samples, or during nonoxidizing silicon processes, when the material thickness is down to 1 nm.

We have shown by the simulation that the concentration of ^{28}SiO generated at the $^{28}\text{Si}/^{28}\text{SiO}_2$ interface and diffusing to the ^{30}Si region critically determines the ^{30}Si self-diffusion. Furthermore, we found in the simulation that the ^{28}SiO concentration in the ^{30}Si region becomes higher at longer annealing times until it reaches the maximum concentration. The simulation results for the 300-nm-thick sample at 1250°C for 6 and 24 h are shown in Fig. 3. The self-diffusivities, assuming a constant diffusion coefficient, show an enhancement of a factor of 4 and are $1 \times 10^{-17} \text{ cm}^2/\text{s}$ for 6 h and $4 \times 10^{-17} \text{ cm}^2/\text{s}$ for 24 h. This time dependence arises because the SiO diffusion is so slow that more ^{28}SiO molecules are arriving from the interface with time, and the self-diffusivity, assuming a constant diffusion coefficient, therefore increases for a longer annealing time. In order to confirm this prediction, we performed an experiment for the time dependence. The results for the 300-nm-thick sample are shown in Fig. 3. The simulated and experimental profiles almost coincide and this confirms the validity of our model. We mention that the simulated results were obtained using the same parameter values for both annealing times. The time-dependent diffusivity was also observed for the 200-

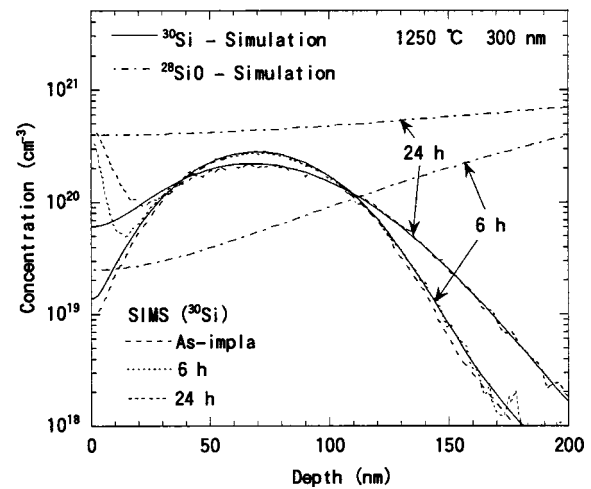


FIG. 3. Simulated and experimental ^{30}Si depth profiles and simulated ^{28}SiO profiles in the 300-nm-thick sample after annealing of 6 and 24 h at 1250°C . The self-diffusivity, assuming a constant diffusion coefficient, shows time dependence, that is, $1 \times 10^{-17} \text{ cm}^2/\text{s}$ for 6 h and $4 \times 10^{-17} \text{ cm}^2/\text{s}$ for 24 h.

nm-thick sample after the same annealing and after 72 and 168 h at 1200°C . For both cases, the experimental profiles were also fitted by using the consistent set of parameters. In the previous studies on Si self-diffusion in SiO_2 , the effect of the Si/SiO_2 interface has not been taken into account and the diffusivity has been obtained assuming a constant diffusion coefficient. However, as shown in this study, the self-diffusivity depends on annealing times and SiO_2 thickness and is described by a modified Eq. (7), $D_{\text{Si}}^{\text{SD}} = D_{\text{Si}}^{\text{SD}}(t_{\text{th}}) + D_{\text{SiO}}^{\text{SD}} C_{\text{SiO}}(x, t) / C_{\text{SiO}}^0$, which depends on x (depth) and t (time). This means that fittings assuming a constant diffusion coefficient are physically unreasonable. In this context, the present work should be regarded as theoretical and experimental evidence of time-dependent self-diffusivity in SiO_2 .

The work was supported in part by a Grant-in-Aid for Scientific Research No. 14076215 and 14550020.

- ¹S. Fukatsu, T. Takahashi, K. M. Itoh, M. Uematsu, A. Fujiwara, H. Kageshima, Y. Takahashi, K. Shiraishi, and U. Gösele, *Appl. Phys. Lett.* **83**, 3897 (2003).
- ²T. Takahashi, S. Fukatsu, K. M. Itoh, M. Uematsu, A. Fujiwara, H. Kageshima, Y. Takahashi, and K. Shiraishi, *J. Appl. Phys.* **93**, 3674 (2003).
- ³D. Tsoukalas, C. Tsamis, and P. Normand, *J. Appl. Phys.* **89**, 7809 (2001).
- ⁴D. Mathiot, J. P. Schunck, M. Perego, M. Fanciulli, P. Normand, C. Tsamis, and D. Tsoukalas, *J. Appl. Phys.* **94**, 2136 (2003).
- ⁵T. Y. Tan and U. Gösele, *Appl. Phys. Lett.* **40**, 616 (1982).
- ⁶G. K. Celler and L. E. Trimble, *Appl. Phys. Lett.* **54**, 1427 (1989).
- ⁷A. M. Stoneham, C. R. M. Grovenor, and A. Cerezo, *Philos. Mag. B* **55**, 201 (1987).
- ⁸Y. Takakuwa, M. Nihei, and N. Miyamoto, *Appl. Surf. Sci.* **117/118**, 141 (1997).
- ⁹H. Kageshima and K. Shiraishi, *Phys. Rev. Lett.* **81**, 5936 (1998).
- ¹⁰H. Kageshima, K. Shiraishi, and M. Uematsu, *Jpn. J. Appl. Phys., Part 2* **38**, L971 (1999).
- ¹¹R. Jaccodine, *Mater. Res. Soc. Symp. Proc.* **716**, 59 (2002).
- ¹²A. M. Agarwal and S. T. Dunham, *J. Appl. Phys.* **78**, 5313 (1995).
- ¹³H. Bracht, N. A. Stolwijk, and H. Mehrer, *Phys. Rev. B* **52**, 16542 (1995).
- ¹⁴W. Jüngling, P. Pichler, S. Selberherr, E. Guerrero, and H. W. Pötzl, *IEEE Trans. Electron Devices* **32**, 156 (1985).
- ¹⁵G. Brebec, R. Seguin, C. Sella, J. Bevenot, and J. C. Martin, *Acta Metall.* **28**, 327 (1980).
- ¹⁶O. Jaoul, F. Béjina, F. Élie, and F. Abel, *Phys. Rev. Lett.* **74**, 2038 (1995).
- ¹⁷D. Tsoukalas, C. Tsamis, and J. Stoemenos, *Appl. Phys. Lett.* **63**, 3167 (1993).